Int. J. Heat Mass Transfer. Vol. 36, No. 4, pp. 1085–1095, 1993
Printed in Great Britain

0017–9310/93 $6.00 + 0.00
Pergamon Press Ltd

Calculation of turbulent flow and heat transfer in a tube with a periodically varying cross-section

L. I. SHUB

North-West Correspondence Polytechnical Institute, St. Petersburg, 195000, Russia

(*Received* 10 *January* 1991)

Abstract—Consideration is given to a developed turbulent flow in a circular tube with an infinite sequence of circumferential fins formed by equidistant diaphragms. For describing the turbulent flow, use is made of the two-parametric dissipative model of turbulence and of the wall function method. Numerical calculation of flow parameters and temperature is based on the computational procedure suggested earlier. The computational algorithm is modernized so that it allows a direct employment of Reynolds number as an input parameter rather than its determination from the predicted results, as is the case in the above-mentioned procedure. A new algorithm to solve the thermal problem is proposed. The calculated results are presented in the form of flow and temperature fields and distributed parameters over the tube surface. The influence of geometry and flow parameters on the dynamic and thermal characteristics of the flow are analyzed.

INTRODUCTION

THERE exist numerous examples of using channels with streamwise periodic variations in the cross-sectional area. The flows in such channels are encountered in heat exchangers, in hydropneumotransport systems, in the technology of manufacturing semiconducting instruments and microcircuits, in labyrinth packing and lubrication devices, and in other technical applications. Some cases of calculating periodic laminar flows are presented in refs. [1–4]. The prediction of a turbulent flow in a tube with a coaxial system of discs is reported in ref. [5]. As regards heat exchangers, of considerable interest is a flow in a channel with a system of flat fins located along the heat transfer surface and oriented perpendicularly to the flow, or a flow in a tube with a system of circumferential fins–diaphragms located uniformly along the flow axis x.

Let us consider some special features of the problem of calculating periodic flows. With L to denote the distance between the fins–diaphragms, the condition of periodicity in the variations of the cross-sectional area will be written as

$$A(x) = A(x+L) = A(x+2L) = \cdots.$$

Here $A(x) = \pi R^2$ holds for the entire tube except for the sections with diaphragms in which $A(x_d) = \pi R^2 \theta^2$ where $\theta = R/R_d$, R_d is the inner radius of a diaphragm.

A distinctive feature of periodic flows is the absence of parabolic properties characteristic of a developed tube flow. Instead of this property, periodicity conditions appear which consist in the fact that the velocity field is the same in the sections distant L apart:

$$u(x,y) = u(x+L,y) = u(x+2L,y) = \cdots,$$

$$v(x,y) = v(x+L,y) = v(x+2L,y) = \cdots.$$

The pressure variation is of dual character. On the one hand, the directed character of flow stipulates, on the average, a linear lengthwise decrease in pressure, while, on the other hand, the elliptical properties of flow within a periodic module of length L induce the pressure variation along the radius in each flow section. The above circumstance enables the representation of pressure as a sum of two terms:

$$p(x,y) = -\beta x + P(x,y). \tag{1}$$

Here, the quantity β is controlled by the integral flow rate in the tube, whereas the function $P(x,y)$, associated with the local motion, is governed by the same conditions of periodicity as the velocity components

$$P(x,y) = P(x+L,y) = P(x+2L,y) = \cdots.$$

The method for predicting periodic flows with reference to a laminar flow was worked out by Patankar *et al.* [6]. The method can be applied for two ways of non-dimensionalization connected with the choice of characteristic velocity. In the first of them, the characteristic velocity is taken to be the quantity ν/R and dimensionless variables are introduced by the equations

$$\bar{u}, \bar{v} = (u^*, v^*)(R/\nu); \quad \bar{P} = P^*(R^2/\nu^2);$$

$$\bar{\beta} = \beta^*(R^3/\rho\nu^2); \quad \bar{k} = k^*(R^2/\nu^2);$$

$$\bar{\varepsilon} = \varepsilon^*(R^4/\nu^3). \tag{2}$$

Here and hereafter, the superscript (*) denotes dimensional quantities. With the non-dimensionalization employed, the transfer coefficient in the momentum equations is determined by the relation $\Gamma = 1 + \nu_t/\nu$. The dimensionless pressure gradient $\bar{\beta}$ is a parameter of the problem. The Reynolds number based on the mean flow velocity, $Re = u^*R/\nu$, is a dependent quan-

NOMENCLATURE

A cross-sectional area
a^{ψ}, b coefficients of discrete equations (10), (18)
c_1, c_2, c_v coefficients in approximated turbulent transport equations
c_p specific heat at constant pressure
E constant in near-wall, $E = 8.8$
F turbulent energy generation rate
G relative decrease in mean-weighted temperature of module
h local heat transfer coefficient, $q(T_{2w} - T_b)$
k turbulent kinetic energy
L dimensionless pitch of fins, L^*/R
Nu local Nusselt number, hR/λ
P periodic pressure
q wall heat flux
R tube radius
R_d inner radius of circumferential fin (diaphragm)
Re Reynolds number in tube flow based on bulk velocity and tube radius, u^*R/ν
S source terms
$T(x, y)$ dimensional temperature
$T_b(x)$ mean-weighted temperature in cross-section
x, y axial and radial coordinate, respectively
u, v dimensionless velocity component along axes x, y, respectively
u^*, v^*, p^*, β^*, k^*, ε^*, L^*, x^* dimensional parameters
$\bar{u}$, $\bar{v}$, $\bar{P}$, $\bar{\beta}$, $\bar{k}$, $\bar{\varepsilon}$, $\bar{L}$, $\bar{x}$ dimensionless quantities introduced by formulae (2)
$\hat{u}$, $\hat{v}$, $\hat{P}$, $\hat{\beta}$, $\hat{k}$, $\hat{\varepsilon}$, $\hat{L}$, $\hat{x}$ dimensionless quantities introduced by formulae (3)
vol_p control volume.

Greek symbols
β averaged pressure gradient, equation (4)
Γ effective diffusion coefficient
Γ_θ effective thermal diffusion coefficient
ΔA side area of control volume
ε dissipation rate of turbulent kinetic energy
θ relative size of fin, R_d/R
θ dimensionless temperature, equation (12)
κ von Karman constant
λ thermal conductivity of fluid
Λ dimensionless mean-weighted temperature gradient
ν kinematic viscosity coefficient
ρ density
σ_k, σ_ε effective turbulent Prandtl number for k and ε, respectively
ϕ dependent variables (u, v, k, and ε).

Superscripts
* preliminarily predicted values
(′), (″) correction parameters.

Subscripts
av cross-section values
P, E, W, N, S values at grid nodes
t turbulent quantities
w wall.

tity and is found from the predicted values of the velocity

$$Re = \int_0^1 \bar{u}^0 y^0 \, dy = \bar{u}_{av}.$$

The conversion into the quantities non-dimensionalized through the division by the mean flow velocity is performed by the relations

$$\beta = \bar{\beta}/Re^2; \quad u = \bar{u}/Re; \quad v = \bar{v}/Re; \quad P = \bar{P}/Re^2;$$
$$k = \bar{k}Re^2; \quad \varepsilon = \bar{\varepsilon}/Re^3; \quad \nu_t = \bar{\nu}_t/Re.$$

The other method of non-dimensionalization involves the selection of the quantity $(\beta^*R/\rho)^{1/2}$ as the characteristic velocity. In this case, the dimensionless averaged pressure gradient becomes equal to unity, $\hat{\beta} = 1$. The rest of the dimensionless variables are introduced with the aid of the relations

$$\hat{u}, \hat{v} = (u, v^*)/(\beta^*R/\rho)^{1/2}; \quad \hat{P} = P^*/(\beta^*R/\rho);$$
$$\hat{k} = k^*/(\beta^*R/\rho); \quad \varepsilon = \varepsilon^*/((\beta^*R/\rho)^{3/2}/R). \quad (3)$$

The independent parameter is the modified Reynolds number $\widehat{Re} = (\beta^*R/\rho)^{1/2}R/\nu$. The dynamic transfer coefficient is determined by the relation $\Gamma = 1/\widehat{Re}(1 + \nu_t/\nu)$.

The equations which are used for conversion into the parameters non-dimensionalized through division by the mean flow velocity, have the form

$$Re = \widehat{Re}\, 2\int_0^1 uy \, dy = \widehat{Re}\, \hat{u}_{av}; \quad \beta = 1/\hat{u}_{av}^2;$$
$$u = \hat{u}/\hat{u}_{av} = \hat{u}\beta^{1/2}; \quad v = \hat{v}\beta^{1/2}; \quad P = \hat{P}\beta;$$
$$k = \hat{k}\beta; \quad \varepsilon = \hat{\varepsilon}\beta^{9/2}; \quad \nu_t = \hat{\nu}_t\beta^{1/2}.$$

In both of these cases of non-dimensionalization, either the standard algorithm SIMPLE or its revised version is used to calculate the fields of the velocities u, v and the function of the pressure P.

Obviously, the method based on computation from the quantities, that have no clear physical meaning, with a subsequent conversion into the traditional vari-

ables is practically inconvenient. Moreover, there is a certain difficulty in selecting the input parameter $\hat{\beta}$ or $\widehat{Re}$ in order to obtain the desired Reynolds number. Following is the method of solution which employs a natural non-dimensionalization of variables through division by the characteristic mean flow velocity.

DYNAMIC PROBLEM

The periodic character of the flow makes it possible to restrict the study to the flow within a single periodic module of the axial size L. As a computational domain, use will be made of the region confined between the axis, tube wall and two sections running through the middle of the distance between two successive fins–diaphragms.

Utilizing the k–ε turbulence model in the cylindrical coordinate system, the system of equations will be written as

$$\frac{\partial u}{\partial x}+\frac{1}{y}\frac{\partial yv}{\partial y}=0, \tag{4}$$

$$\frac{1}{y}\left\{\frac{\partial}{\partial x}\left[y\left(u^2-\Gamma\frac{\partial u}{\partial x}\right)\right]+\frac{\partial}{\partial y}\left[y\left(uv-\Gamma\frac{\partial u}{\partial y}\right)\right]\right\}=\beta-\frac{\partial P}{\partial x}+S_u, \tag{5}$$

$$\frac{1}{y}\left\{\frac{\partial}{\partial x}\left[y\left(uv-\Gamma\frac{\partial v}{\partial x}\right)\right]+\frac{\partial}{\partial y}\left[y\left(v^2-\Gamma\frac{\partial v}{\partial y}\right)\right]\right\}=-\frac{\partial P}{\partial y}+S_v, \tag{6}$$

$$\frac{1}{y}\left\{\frac{\partial}{\partial x}\left[y\left(uk-\frac{\nu_t}{\sigma_k}\frac{\partial k}{\partial x}\right)\right]+\frac{\partial}{\partial y}\left[y\left(vk-\frac{\nu_t}{\sigma_k}\frac{\partial k}{\partial y}\right)\right]\right\}=S_k, \tag{7}$$

$$\frac{1}{y}\left\{\frac{\partial}{\partial x}\left[y\left(u\varepsilon-\frac{\nu_t}{\sigma_\varepsilon}\frac{\partial \varepsilon}{\partial x}\right)\right]+\frac{\partial}{\partial y}\left[y\left(v\varepsilon-\frac{\nu_t}{\sigma_\varepsilon}\frac{\delta \varepsilon}{\delta y}\right)\right]\right\}=S_\varepsilon, \tag{8}$$

where $\Gamma=1/Re+\nu_t$ is the transfer coefficient and $\nu_t=c_\nu k^2/\varepsilon$ is the eddy viscosity.

The source terms are obtained from the equations

$$S_u=\frac{\partial}{\partial x}\left(\Gamma\frac{\partial u}{\partial x}\right)+\frac{1}{y}\frac{\partial}{\partial y}\left(y\Gamma\frac{\partial v}{\partial x}\right);$$

$$S_v=\frac{\partial}{\partial x}\left(\Gamma\frac{\partial u}{\partial y}\right)+\frac{1}{y}\frac{\partial}{\partial y}\left(y\Gamma\frac{\partial v}{\partial y}\right)-2\Gamma\frac{v^2}{y^2};$$

$$S_k=F-\varepsilon;\quad S_\varepsilon=\frac{\varepsilon}{k}(c_1F-c_2\varepsilon);$$

$$F=\Gamma\left\{2\left[\left(\frac{\partial u}{\partial x}\right)^2+\left(\frac{\partial v}{\partial y}\right)^2+\left(\frac{v}{y}\right)^2\right]+\left(\frac{\partial u}{\partial y}+\frac{\partial v}{\partial x}\right)^2\right\}.$$

The following values of the turbulence constants are adopted: $c_\nu=0.09$, $c_1=1.44$, $c_2=1.92$, $\sigma_k=1.0$, and $\sigma_\varepsilon=1.3$.

In writing the equations, the linear dimensions x, y, L are related to the tube radius R and the velocities u, v are related to the mean mass velocity u^*_{av}. The local pressure P, the averaged longitudinal pressure gradient β, the transfer coefficient Γ, the turbulent energy k, and the dissipation rate of turbulent energy ε are normalized, by ρu^{*2}_{av}, $\rho u^{*2}_{av}/R$, $u^*_{av}R$, u^{*2}_{av}, $\rho u^{*3}_{av}/R$, respectively.

The system of equations is solved under the following periodicity conditions:

$$\phi(0,y)=\phi(L,y),\quad \phi=u,v,P,k,\varepsilon;$$

conditions on the symmetry axis:

$$v=0;\quad \partial\phi/\partial y=0,\quad \phi=u,P,k,\varepsilon$$

and under the boundary conditions on the solid walls formulated by the wall function method.

To determine the coefficient β, the integral continuity equation is used

$$\int_0^1(1-u)y\,dy=0, \tag{9}$$

which can be controlled in an arbitrary cross-section of the module.

Finite-difference equations are set up by the control volume method, as a result of which the differential transfer equations are reduced to an algebraic form

$$a^\phi_P\phi_P=a^\phi_E\phi_E+a^\phi_W\phi_W+a^\phi_N\phi_N+a^\phi_S\phi_S+s_\phi, \tag{10}$$

where the coefficients a^ϕ and the source term s_ϕ are evaluated, depending on the adopted approximation of convection and diffusion terms, by the best, known at this time, grid parameters from the previous iteration scheme. In the bordering volumes, the flow on the edges coinciding with the symmetry axis goes to zero, whereas that on the edges that lie on the solid walls is found by the wall function method, viz.:

the diffusion flux to the wall is determined in accordance with the expression

$$\left(\Gamma\frac{\partial u}{\partial n}\right)_w=\kappa u_P c_\nu^{1/4}k_P^{1/2}/\ln(Ey_PRe\,c_\nu^{1/4}k_P^{1/2})$$

where y_P is the distance from the node to the wall, $\kappa=0.4$ and $E=8.8$ are constants in the logarithm of the velocity;

the turbulent kinetic energy diffusion flux to the wall is assumed to be equal to zero ($\Gamma_k\,\partial k/\partial n)_w=0$, whereas the source term is determined from the equation

$$\int_0^{y_P}\varepsilon\,dy=c_\nu^{3/4}k_P^{9/2}/\kappa\ln(Ey_PRe\,c_\nu^{1/4}k_P^{1/2});$$

the turbulent kinetic energy dissipation rate is

obtained according to the expression

$$\varepsilon_P = c_\nu^{1/4} k_P^{9/2}/(\kappa y_P).$$

The solution algorithm is set up by the SIMPLE method or its modification [4] the procedure of which is changed to suit the need for identifying the coefficient β in momentum equation (5).

Let u^*, v^*, P^*, and β^* be the best known values of the velocity, elliptical pressure component, and of the streamwise pressure gradient at a given iteration step. The indicated grid values are corrected in such a way as to satisfy continuity equations in differential (4) and integral (10) forms. For this purpose, the correction relations are introduced:

$$u = u^* + u' + u''; \quad v = v^* + v'; \quad P = P^* + P';$$
$$\beta = \beta^* + \beta'.$$

The introduction of two corrections for the streamwise velocity component reflects the dual character of the flow being formed by the action of both specified averaged translational and local disturbances associated with periodic variations in the flow cross-sectional area. Just as in standard SIMPLE-type procedures, the velocity corrections u' and v' are expressed in terms of the appropriate differences of the corrections of the pressure component P', which, in turn, are found from the Poisson difference equation. The second velocity correction u'' is calculated in terms of the correction to the gradient of the linear pressure component β': $u'' = \mathrm{vol}_P/a_P^u \beta'$. The relation defining β' is obtained by writing integral equation (9) in the difference

$$\beta' = \sum[(1-u_P^*)\Delta A]/\sum\left(\frac{\mathrm{vol}_P}{a_P^u}\Delta A\right),$$

in which the summation is taken over all the nodes lying in the section chosen to check equation (9). Here, vol_P is the control volume and ΔA is the area of the control volume side in the lateral direction.

THERMAL PROBLEM

The temperature field is determined by solving the energy equation

$$\rho c_p\left(\frac{1}{y}\frac{\partial yvT}{\partial y} + \frac{\partial uT}{\partial x}\right) = \frac{1}{y}\frac{\partial}{\partial y}\left(y\lambda_{\mathrm{eff}}\frac{\partial T}{\partial y}\right) + \frac{\partial}{\partial y}\left(\lambda_{\mathrm{eff}}\frac{\partial T}{\partial x}\right), \quad (11)$$

where $\lambda_{\mathrm{eff}} = \lambda + \lambda_t$ is the effective thermal conductivity coefficient.

Let the tube walls be maintained at a constant temperature $T = T_w$. With the heat conduction process in the tube disregarded, the tube will be considered to be in isothermal conditions. For the class of periodic flows (as well as for developed tube flows), the dimensionless temperature is introduced

$$\theta = \frac{T(x,y) - T_w}{T_b(x) - T_w}, \quad (12)$$

which is invariant for a multitude of periodic modules. Here, $T_\sigma(x)$ is the local characteristic temperature taken reasonably to be that averaged over the cross-section with the streamwise velocity module used as a weight function

$$T_b(x) - T_w = \left[\int_0^1 (T - T_w)uy\,dy\right]\Big/\left[\int_0^1 uy\,dy\right]. \quad (13)$$

Passing over in equation (11) to dimensionless variables, the energy equation will be restated as

$$\frac{1}{y}\frac{\partial}{\partial x}\left(u\theta - \Gamma_\theta\frac{\partial\theta}{\partial x}\right) + \frac{\partial}{\partial y}\left[y\left(v\theta - \Gamma_\theta\frac{\partial\theta}{\partial y}\right)\right] = \sigma, \quad (14)$$

where

$$\Gamma_\theta = 1/(Re\,Pr) + \nu_t/Pr_t, \quad Pr = \rho c_p \nu/\lambda,$$
$$Pr_t = \rho c_p \nu_t/\lambda_t,$$
$$\sigma = \left(2\Gamma_\theta\frac{\partial\theta}{\partial x} - u\theta\right)\frac{dT_b(x)/dx}{T_b(x) - T_w} + \frac{\theta}{T_b(x) - T_w}\frac{d}{dx}\left[\Gamma_\theta\frac{dT_b(x)}{dx}\right].$$

Introducing the notation

$$\Lambda(x) = \frac{d[T_b(x) - T_w]/dx}{T_b(x) - T_w}$$

the right-hand side of equation (14) will be written in the form

$$\sigma = \left\{\Gamma_\theta\left[\frac{\partial\Lambda}{\partial x} + \Lambda^2\right] + \Lambda\frac{\partial\Gamma_\theta}{\partial x} - u\Lambda\right\}\theta + 2\Gamma_\theta\Lambda\frac{\partial\theta}{\partial x}. \quad (15)$$

Periodic changes in the variables θ and Γ_θ entail periodic variables in the parameters σ and Λ. An additional condition for finding the function Λ is provided by means of integration over the cross-section area of equation (12) which has been multiplied by the velocity modulus u. In view of equation (13), the resultant relation is represented as

$$\int_0^1 \theta uy\,dy = \int_0^1 uy\,dy. \quad (16)$$

Equations (14) with the right-hand sides of equations (15) and (16) serve for determining two unknown variables, viz. the dimensionless temperature θ and the specific longitudinal gradient of the mean-weighted temperature Λ.

The statement of the boundary conditions for the temperature θ reduces to a situation when, in integrating over the control volume during the numerical scheme construction, the temperature gradient on the

side coinciding with the wall is defined by the relation

$$\left(-\Gamma_\theta \frac{\partial \theta}{\partial y}\right)_w = \frac{c_\nu^{1/4} k_P^{1/2} \theta_P}{F_P}$$

for the horizontal walls and

$$\left[-\Gamma_\theta \left(\frac{\partial \theta}{\partial x} + \theta \Lambda\right)\right]_w = \frac{c_\nu^{1/4} k_P^{1/2} \theta_P}{F_P}$$

for the vertical walls, where

$$F_P = Pr_t \ln (E y_P Re\, c_\nu^{1/4} k_P^{1/2})/\kappa + f(\Pi),$$

$$f(\Pi) = 9.24(\Pi^{3/4} - 1)[1 + 0.28 \exp(-0.007\Pi)],$$

$$\Pi = Pr/Pr_t.$$

To simultaneously solve equations (14) and (16), the algorithm can be used which was proposed in ref. [6] but somewhat modified to take into account the features of turbulent flow equations. Another algorithm can also be suggested, which is constructed similarly to the SIMPLE algorithm for the dynamic problem in the following manner:

1. First, the grid temperature values are determined from equation (14), the right-hand side of which is calculated from the best known values of the function Λ^*. The resulting temperature values are regarded as tentative and are denoted by θ^*.

2. The actual values of the temperature θ and function Λ are related to the tentative values by the equations

$$\Lambda_P = \Lambda_P^* + \Lambda_P'; \quad \theta_P = \theta_P^* + \theta_P', \tag{17}$$

where θ' is expressed in terms of Λ' according to the finite-difference scheme obtained from equation (14)

$$\theta_P' = b_P \Lambda_P' + b_E \Lambda_E' + b_W \Lambda_W' + Q_\Lambda. \tag{18}$$

In setting up equation (18), the terms involving the temperature values at adjoining nodes in the difference analogue of equation (14) are discarded ($\Sigma_{i=E,W,N,S} a_i^\theta \theta_i = 0$). The coefficients in equation (18) are computed from the grid values of θ^* and Λ^*.

3. A difference analogue is set up to determine the correction function Λ'. To this end, the values of θ from equation (17) are substituted into equation (16) with allowance for equation (18). This yields the relation

$$\Lambda_P' \int b_P^u \, dA = \Lambda_E' \int b_E^u \, dA + \Lambda_W^u \int b_W^u \, dA + \int Q_\Lambda \, dA + \int (1 - \theta^*) u \, dA, \tag{19}$$

in which integration is carried out over the flow cross-section. Equation (19) is of standard three-point form. It is solved through a periodic factorization by the algorithm stated in ref. [6].

4. The obtained values of Λ' are employed to correct the values of Λ and θ at the given iteration step in accordance with expressions (17) and (18).

CALCULATED RESULTS

Dynamic problem

The flow pattern in a tube with annular fins–diaphragms is governed by three criteria: the Reynolds number $Re = u_{av}^* R/\nu$, the relative diameter of the annular diaphragm $\theta = R_d/R$, and the relative fin spacing $L = L^*/R$. Calculations were performed for the fixed Reynolds number $Re = 10^5$ and varied values of the geometric parameters: $\theta = 0.9$ and $\theta = 0.8$, $L = 1.5$, $L = 1.0$, $L = 0.6$, and $L = 0.3$.

The flow character is defined by the stream-function fields plotted in Fig. 1. The presented field fragments reflect the flow pattern in the near-wall region where the maximum flow deformation occurs owing to the flow past the fin. In the axial region, the streamlines actually remain straight just as in undisturbed tube flow and therefore they are not given in the figures. The flow characteristics in the near-wall region are determined by the fin size $1-\theta$ and the fin spacing L. A stalling flow past the fin in the near wake is accompanied by the formation of a toroidal vortex. In the case of small relative fin sizes $(1-\theta)/L < 0.07$, the flow in the stalling zone is similar to the flow past a single fin. The effect of the fin situated downstream is virtually negligible (Fig. 1(a)). The vortex flow intensity, which can be inferred from the maximum stream function value at the vortex centre, is mainly governed by the fin size $1-\theta$ and is little dependent on the fin spacing L. A decrease in the fin spacing L activates a vortex motion in the stagnant zone ahead of the fin (Figs. 1(b), (e)). The vortex intensity and size increase with the decrease in L (see Fig. 1(c)) and, when $(1-\theta)/L > 0.2$–0.25, the two vortexes in the stalling and stagnant zones converge (Figs. 1(d), (f), (g), (h)). For small relative fin pitches $(1-\theta)/L > 0.3$ (Figs. 1(d), (g), (h)), the entire flow can be conventionally divided into two parts: a vortex flow in the annular space bounded by the tube surface and coaxial cylindrical surface enveloping the fin edges and a smooth flow in the cylindrical axial region. In the latter region, the flow resembles that in a tube of diameter $1-\theta$: the warping of streamlines near the fin edges is insignificant.

Consider the distribution patterns of the turbulence parameters κ and ε in the field of the calculated module in Figs. 2 and 3. The fin edge is a source of intense turbulent disturbances. Close to the fin edge, the peak of the turbulent energy k is produced which shifts upwards to the edge tip as the fin spacing L decreases. Relative to the undisturbed tube flow, the value of k_{max} grows by a few tens of times. The value of k_{max} within the range of sizes under study increases almost proportionally to the fin height. At the same time, a variation in the fin spacing affects k_{max} little. An intense flow turbulization causes an increase of the turbulent viscosity ν_t. The turbulent viscosity isolines in the flow region, given in Fig. 3, reveal that, except for the fin edge and stalling flow region, the character of the turbulent viscosity alteration remains the same

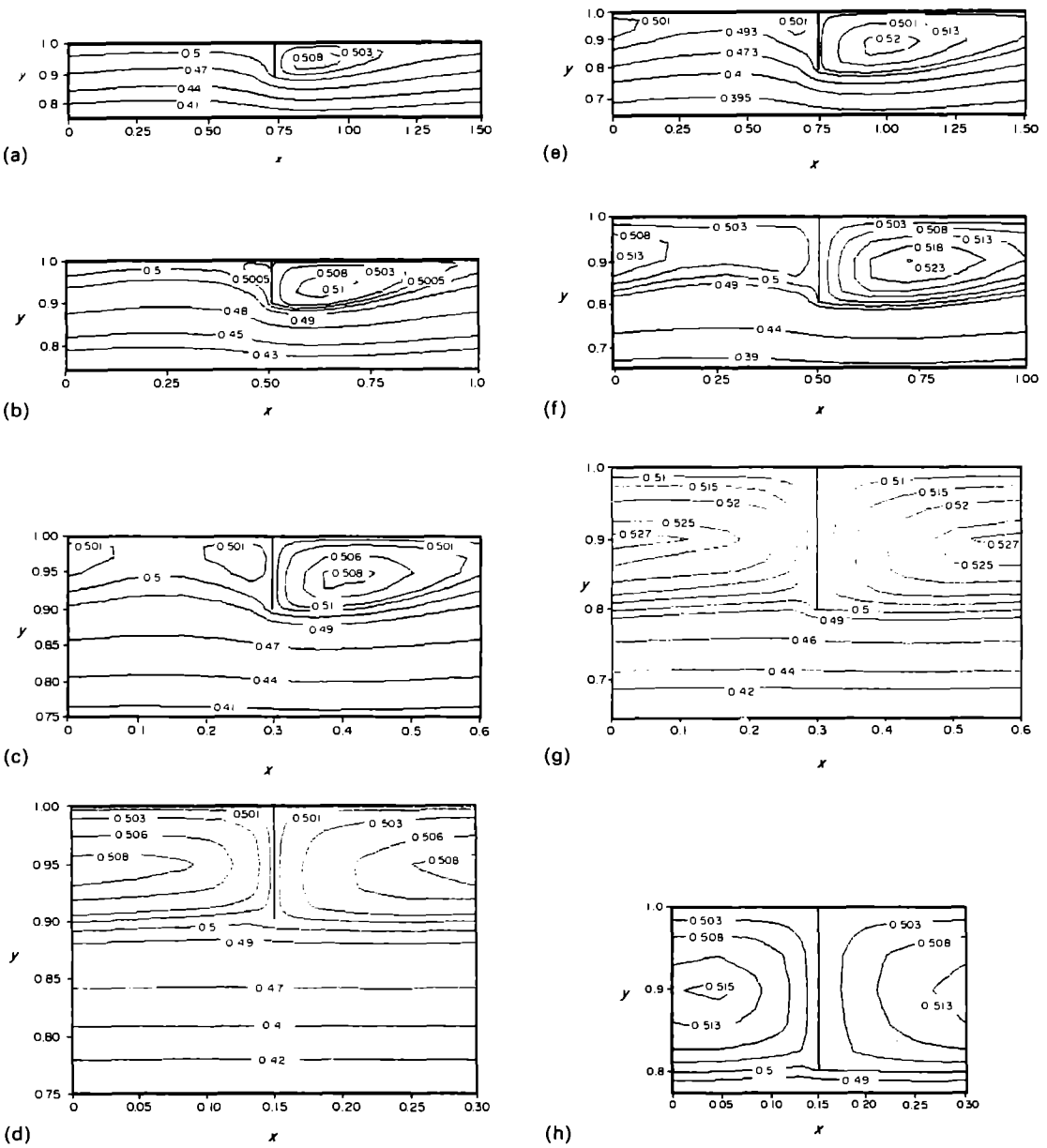

FIG. 1. The streamlines ψ in the field of the calculated module for various fin sizes θ and fin spacings L: a, b, c, d—$\theta = 0.9$; e, f, g, h—$\theta = 0.8$; a, e—$L = 1.5$; b, f—$L = 1$; c, d—$L = 0.6$; d, h—$L = 0.3$.

as that for the flow in a smooth tube. Viscosity increases monotonically from solid surfaces towards the axis. The maximum viscosity $\nu_{t,max}$ is achieved on the flow axis. Just as k_{max}, the value of $\nu_{t,max}$ grows nearly proportionally to the fin size and slightly reduces with a decrease in the fin spacing.

Now, evaluate the hydraulic resistance of a tube with uniformly arranged fins–diaphragms. In a periodic flow the hydraulic resistance is determined by the module-length-averaged dimensionless pressure gradient β. Figure 4(a) plots the relative value of β/β_0 vs the spacing between discs L for two adopted fin sizes. The quantity β_0 denotes the hydraulic resistance coefficient of a smooth tube, which is found from the Blasius equation $\beta_0 = 0.3164/[4(2Re)^{0.25}]$. It must be noted that for $L = 0$ with the non-dimensionalization method assumed, the ratio β/β_0 is defined as $1/\theta^{4.75}$. With increasing L an abrupt rise of hydraulic resistance is observed despite the fact that at small L, as was remarked above, the main flow is deformed little and it is similar to that in a tube of radius decreased by θ times. This is evidently associated with intense flow turbulization on the sharp fin edges. The maximum value of β/β_0 is attained at the relative fin spacing $L/(1-\theta)$ of the order of 7. A further increase in L leads to a gradual decrease in the hydraulic resistance. In order to validate the statement that hydraulic resistance is closely bound up with the flow turbulization on sharp edges, Fig. 4(a) plots the relative increase in the maximum turbulent kinetic energy

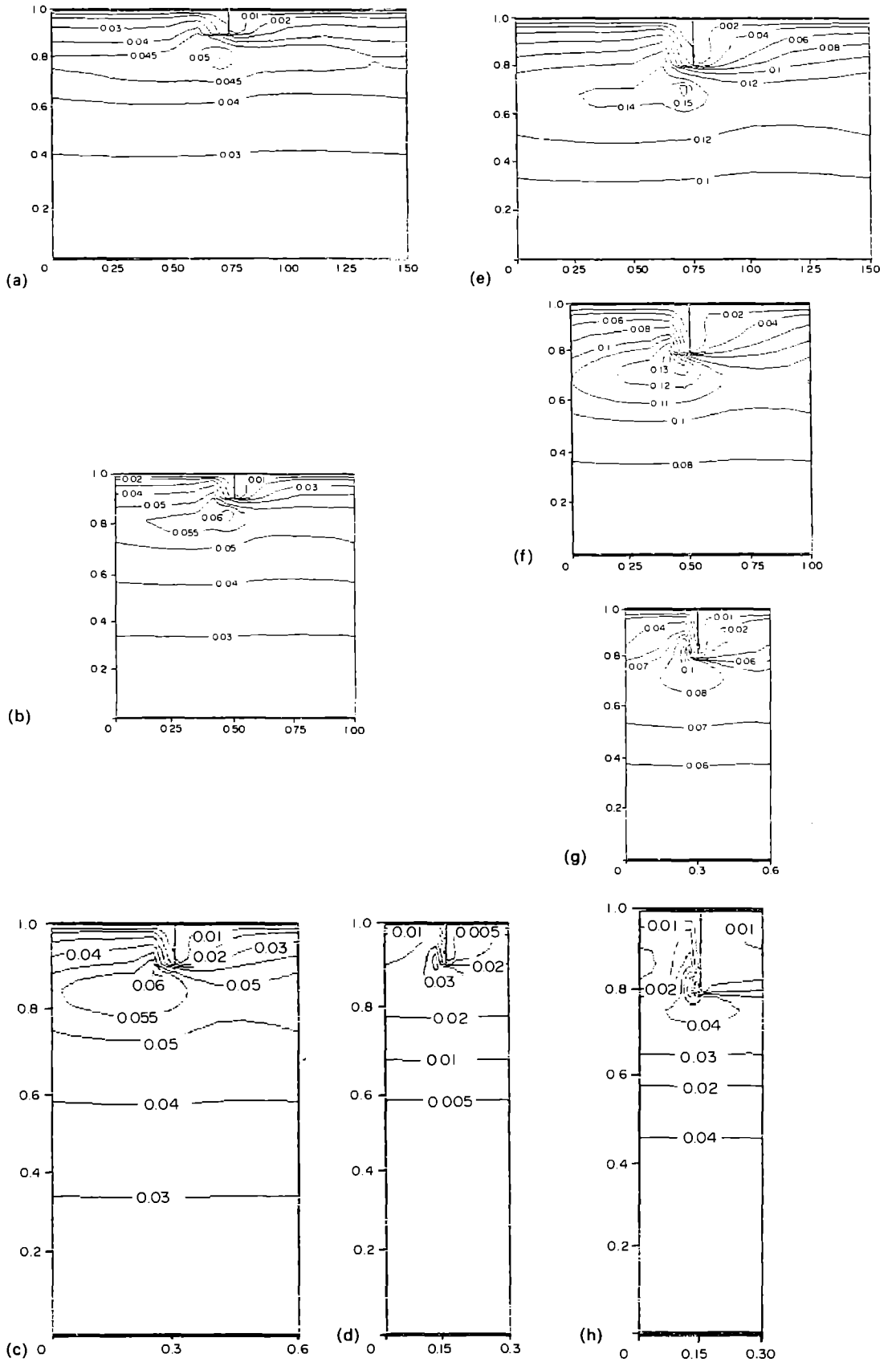

FIG. 2. Distribution of the turbulent kinetic energy k in the field of the calculated module. See notation in Fig. 1.

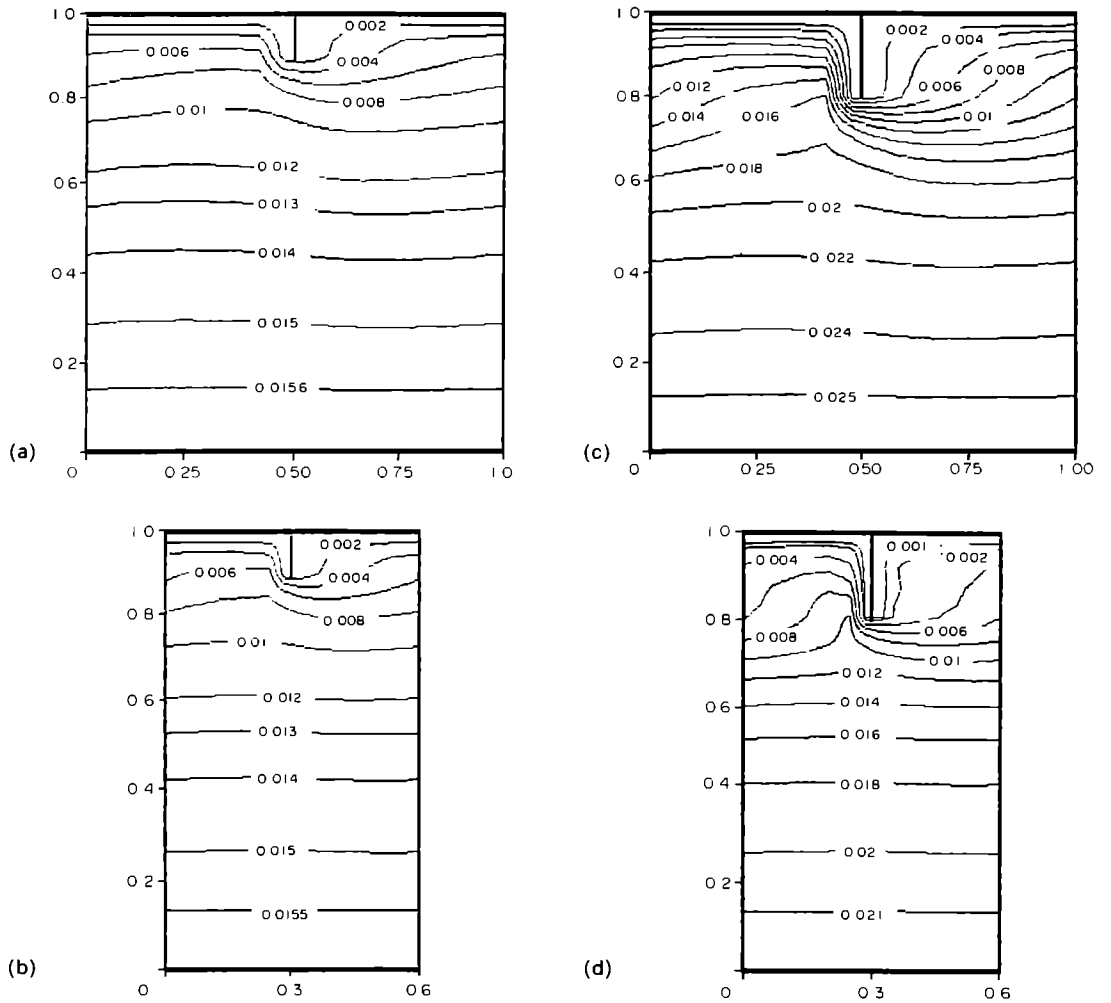

FIG. 3. Isolines of the turbulent viscosity ν_t; a, b—$\theta = 0.9$; c, d—$\theta = 0.8$; a, c—$L = 1.0$; b, d—$L = 0.6$.

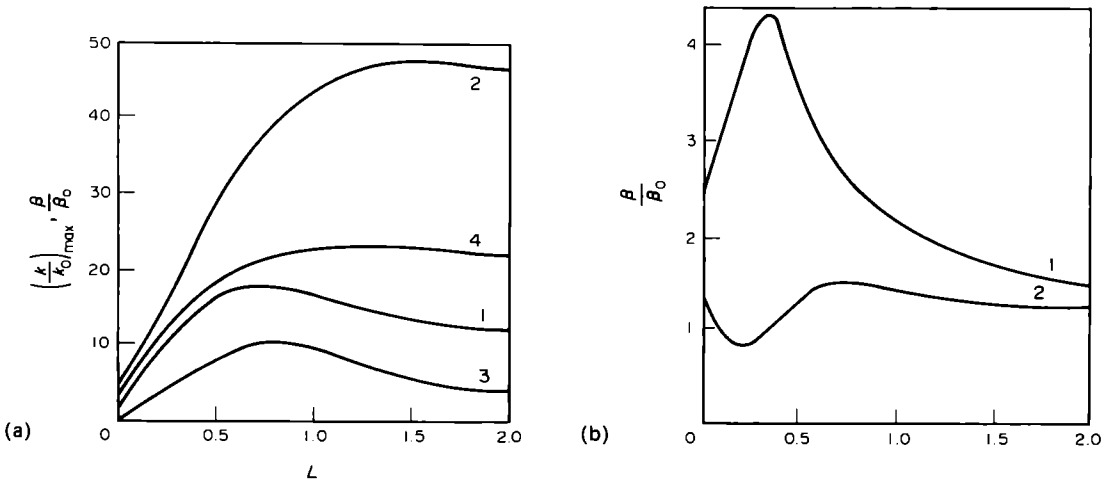

FIG. 4. The relative values of hydraulic resistance of a tube and of the maximum turbulent kinetic energy vs the geometric parameters L and θ: a—$Re = 10^5$; 1, 2—β/β_0; 3, 4—$(k/k_0)_{max}$; 1, 3—$\theta = 0.9$; 2, 4—$\theta = 0.8$; b—$Re = 100$ (laminar flow).

in a finned tubed $(k/k_0)_{max}$. Here $k_{0,max}$ is the maximum turbulent energy in a smooth tube; $k_{0,max} \cong 6.5 \times 10^{-3}$ at $Re = 10^5$. The character of the variation in the curves for β/β_0 and $(k/k_0)_{max}$ is identical.

It is of interest to note that the hydraulic resistance of a tube with fins–diaphragms can possess abnormal properties in the case of a laminar flow. The curves for β/β_0 at $Re = 100$, given in Fig. 4(b), demonstrate that, at some values of θ and L, the hydraulic resistance can even decrease as against that in a smooth tube.

Thermal problem

This section presents the analysis of the impact of the geometric parameters (L and θ) on the thermal characteristics of the flow. Calculations are carried out for a single Reynolds number $Re = 10^5$ and two Prandtl numbers $Pr = 0.7$ and $Pr = 7.0$ typical of air and water.

Figure 5 gives the fields of the dimensionless temperature θ at $Pr = 0.7$ for two values of the geometric parameters L and θ. The isotherms are drawn with equal temperature steps. In the large part of the near-axis flow region, the temperature changes inconsiderably. The greatest temperature deformation of the flow is observed in the vicinity of the wall of the tube and fin in the area of vortex formation. The position of the isotherms shows that the temperature decreases to the utmost on the windward fin side, not so greatly along the tube surface, and the minimum rate of temperature decrease takes place on the leeward fin side; here, in the direction of the fin edge, the temperature gradients on its surface increase. With the variation in

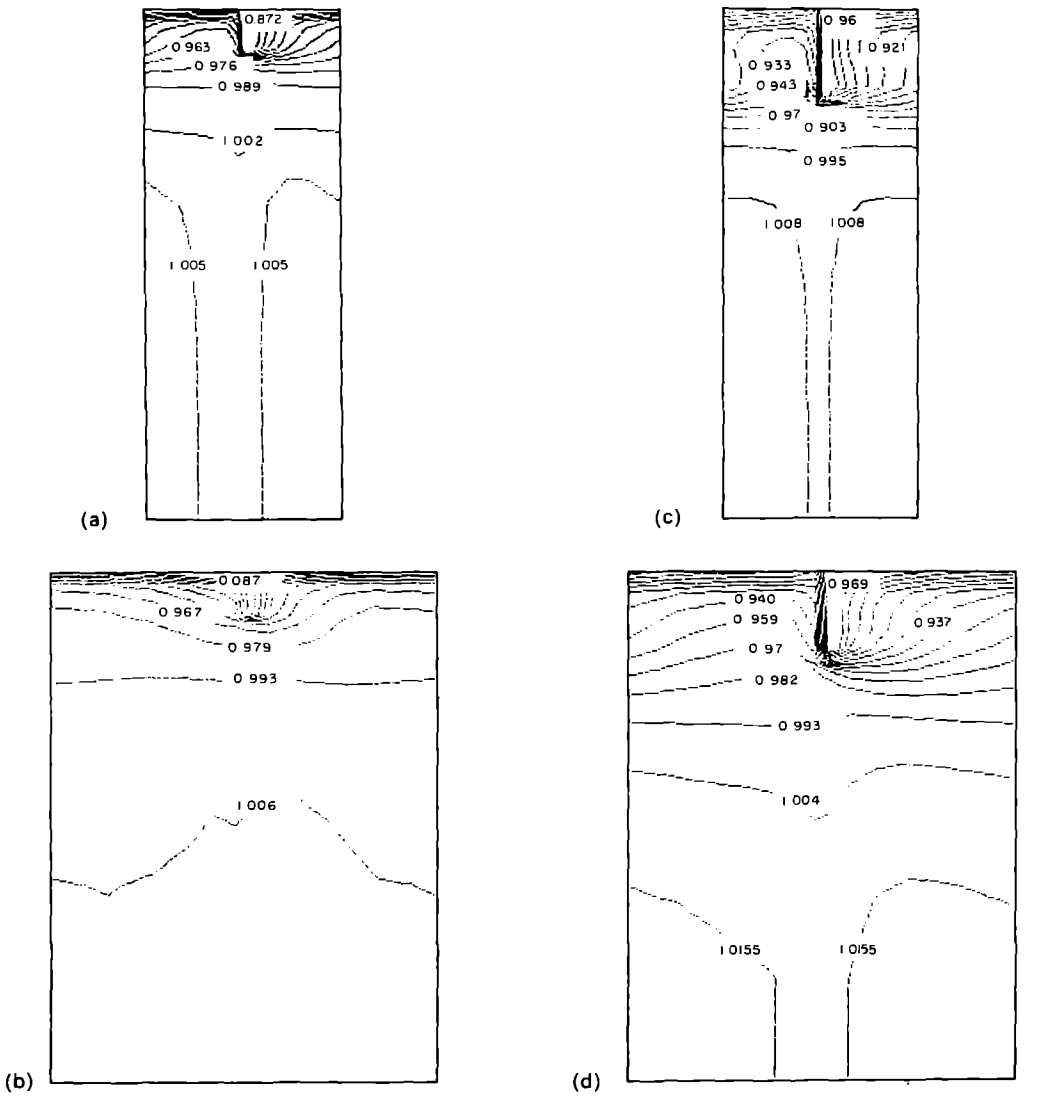

FIG. 5. The fields of the dimensionless temperature θ for the following geometric parameters of the module: a—$\theta = 0.9$, $L = 0.3$; b—$\theta = 0.8$, $L = 0.6$; c—$\theta = 0.8$, $L = 0.3$; d—$\theta = 0.8$, $L = 0.6$.

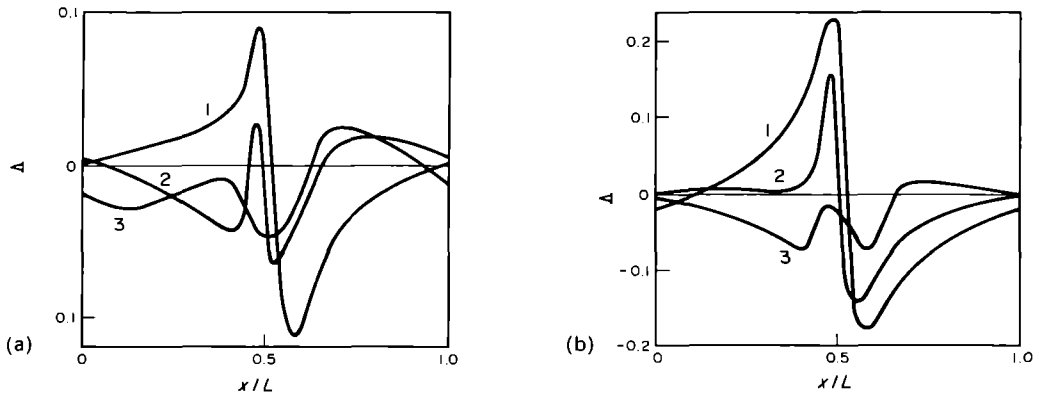

FIG. 6. A variation in the function Λ along the module length: a—$\theta = 0.9$, 1—$L = 0.3$; 2—$L = 0.6$; 3—$L = 1.0$; b—$\theta = 0.8$, 1—$L = 0.3$; 2—$L = 0.6$; 3—$L = 1.5$.

the parameters L and θ, the character of temperature distribution over the near-wall region is maintained. With an increase in the Prandtl number and with the isotherm pattern being preserved, the flow temperature equalization occurs, and the temperature gradients outside the laminar sublayer decrease due to the fact that the role of convective heat transfer becomes more essential.

An idea of the character of variation of the parameter (which is the relative magnitude of the longitudinal gradient of the mean-weighted temperature defect $T_b - T_w$) along the calculated region is given by the plots of Fig. 6. The character of variation of Λ is controlled by the vortex structure of the flow. The value of Λ decreases abruptly in the region of flow separation behind the fin. In the zone, where the flow is attached to the wall, the parameter Λ grows. In this case, with a decrease in the module size and with an increase in the fin size, the non-uniformity of variations in Λ gets more pronounced.

The obtained solution to the energy equation allows a determination of the heat transfer coefficient α, introduced as a ratio of the specific heat flux on the tube surface to the mean-weighted temperature at the given section $\alpha = q_w/(T_w - T_b)$. The dimensionless heat transfer coefficient, i.e. the Nusselt number $Nu = \alpha R/\lambda$, is determined in terms of the dimensionless temperature gradient from the equations

$$Nu = (\partial\theta/\partial y)_w; \quad Nu = (\partial\theta/\partial x + \Lambda\theta)_w$$

for horizontal and vertical surfaces, respectively. Figure 7 plots the variation in the local Nusselt number along the tube surface related to the Nusselt number Nu_0 for the flow in a smooth tube at the same parameters Re and Pr. The latter is obtained from the equation

$$Nu = 0.0115(2Re)^{0.8}Pr^{0.43}.$$

The Nusselt number is minimum in the vicinity of the fin in the stalling zone. In all the variants considered, the relative Nusselt number is smaller than unity. The largest Nu is observed in the region of the flow attachment to the wall. A comparative analysis of the calculated variants disclosed that the maximum enhancement of heat transfer occurs at the fin spacings of the order of 7–8 fin heights, i.e. at the distance approach-

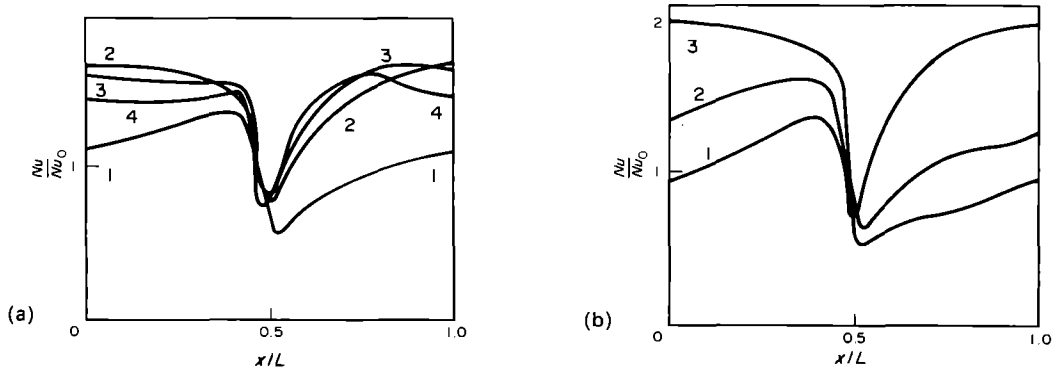

FIG. 7. A variation in the Nusselt number Nu along the tube surface in the calculated module: a—$\theta = 0.9$, 1—$L = 0.3$, 2—$L = 0.6$, 3—$L = 1.0$, 4—$L = 1.5$; b—$\theta = 0.8$, 1—$L = 0.3$, 2—$L = 0.6$, 3—$L = 1.0$.

ing the length of the stalling zone of the flow past a single fin. In this case, the heat transfer enhancement along the module length is, on the average, larger by 1.2 times at $\theta = 0.09$ and by 1.7 times at $\theta = 0.8$ in comparison with a smooth tube. The minimum heat transfer coefficient on the tube surface is characteristic of small fin spacings (curves 1 in Figs. 7(a), (b)). For large fins and small fin spacings, the heat transfer coefficient can become even smaller than that in a smooth tube. It should be noted that the hydraulic resistance excess in the case of a finned tube as compared with a smooth tube is many times larger than the possible heat transfer enhancement in all calculated variants. Self-similarity of the local and module-averaged heat transfer coefficient with respect to the Prandtl number is confirmed by calculations. The Prandtl number exponent in the dimensionless relation is equal to 0.3.

In conclusion, consider the trends of variation of the mean-weighted temperature along the module

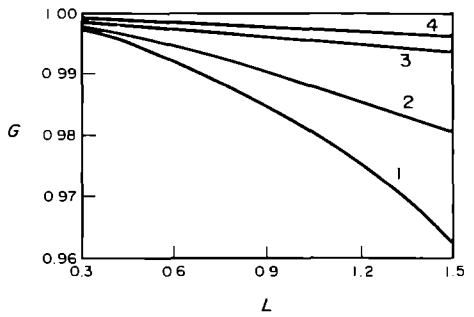

FIG. 8. A variation in the mean-weighted temperature along the module length: 1—$\theta = 0.8$, $Pr = 0.7$; 2—$\theta = 0.9$, $Pr = 0.7$; 3—$\theta = 0.8$, $Pr = 7.0$; 4—$\theta = 0.9$, $Pr = 7.0$.

length, which is determined by the function G:

$$G = (T_b - T_w)_{x=L}/(T_b - T_w)_{x=0}.$$

The value of G is computed in terms of the function Λ from the equation

$$G = \exp\left(\int_0^L \Lambda \, dx\right).$$

Figure 8 presents a plot of G as a function of the fin spacing L. The relative temperature decrease $T_b - T_w$ grows with an increase in L and in the fin size $1 - \theta$, as well as with a decrease in the Prandtl number.

REFERENCES

1. J. Rowlay and S. V. Patankar, Analysis of laminar flow and heat transfer in tubes with internal circumferential fins, *Int. J. Heat Mass Transfer* **27**, 553–560 (1984).
2. B. W. Webb and S. Ramadhyami, Conjugate heat transfer in a channel with staggered ribs, *Int. J. Heat Mass Transfer* **28**, 1679–1687 (1985).
3. A. T. Prata and E. M. Sparrow, Heat transfer and fluid flow characteristic for an annulus of periodically varying cross-section, *Numerical Heat Transfer* **7**, 285–304 (1984).
4. I. A. Belov and L. I. Shub, Study of fluid flow in a pipeline with moving containers based on numerical solution of Navier–Stokes and Reynolds equations. In *Introduction to Aerodynamics of Container Pipe-line Transportation*, pp. 18–40. Izd. Nauka, Moscow (1986).
5. L. I. Shub, Calculation of turbulent vortex structures in a flow past a set of discs in a tube. In *Transfer Processes in Turbulent Flows*, pp. 49–58. Izd. ITMO AN BSSR, Minsk (1988).
6. S. V. Patankar, *Numerical Heat Transfer and Fluid Flow*. Hemisphere Publishing Corporation, New York (1980).
7. S. V. Patankar, C. K. Liu and E. M. Sparrow, Fully developed flow and heat transfer in ducts having streamwise-periodic variations of cross-section area, *J. Heat Transfer* **99**, 180–186 (1977).